Microchimica Acta (2019) 186: 291
https://doi.org/10.1007/s00604-019-3379-8

ORIGINAL PAPER

Sensitive determination of nitrite by using an electrode modified with hierarchical three-dimensional tungsten disulfide and reduced graphene oxide aerogel

Xue Ma[1,2] · Feng Gao[1] · Guangbin Liu[1] · Yu Xie[1] · Xiaolong Tu[1] · Yongzhen Li[3] · Runying Dai[1] · Fengli Qu[2] · Wenmin Wang[1] · Limin Lu[1]

Received: 4 January 2019 / Accepted: 21 March 2019 / Published online: 23 April 2019

Abstract

Nanosheets of tungsten disulfide (WS_2) were used to improve the physicochemical properties of reduced graphene oxide aerogel (rGA). The nanosheets were directly integrated into 3D hybrid architecture of rGA by a solvothermal mixing method by which the WS_2 sheets were assembled onto the conductive graphene network. WS_2 with highly exfoliated and defect-rich structure made the WS_2/rGA composite possess plentiful active sites, and this enhanced the electrocatalytic capability of the composite. The introduction of poorly conductive WS_2 into 3D rGA system decreases the background current of rGA when used as electrode material. This is advantageous in terms of signal to-noise ratio and analytical performance in general. The WS_2/rGA electrode, best operated at a potential of 0.68 V (*vs.* SCE) has a linear response in the 0.01 to 130 μM nitrite concentration range with a low detection limit of 3 nM (at $S/N = 3$). It is selective, reproducible, stable and is successfully applied to the determination of nitrite in spiked bacon samples.

Keywords Tungsten disulfide · Physicochemical properties · Reduced graphene oxide aerogel · Modified electrode · Three-dimensional structure · Nitrite · Bacon

Introduction

Nitrite is widely used in the food industry as a food additive to improve the flavor and color of the cured meat. However, excessive consumption would cause nitrite to react with amine in food, producing carcinogenic amine nitrite [1, 2]. In addition, nitrite can cause a decrease in oxygen transport capacity, and then hemoglobin is converted to methemoglobin. Finally, irreversible effects affect human health [3]. Therefore, it is urgent to find an economical and reliable way to detect nitrite. Currently, different methods have been used to the detection of nitrite, such as cloud point extraction spectrophotometry [4], high efficiency liquid chromatography [5], chemiluminescence [6], and electrochemical detection [7]. Among these methods, electrochemical methods have aroused widespread concern owing to their rapid response, high sensitivity, low cost and short time.

Graphene and its composites exhibit good electrochemical performance owing to their superior properties, such as high surface area, good conductivity and chemical stability [8, 9]. However, graphene sheets easily tend to aggregate due to the strong van der Waals force and π interaction, which reduce the effective surface area and the active sites [10]. Graphene aerogel, a novel kind of highly porous three-dimensional (3D) graphene with network structure can inhibit the restacking of individual graphene sheets. It not only maintains

Electronic supplementary material The online version of this article (https://doi.org/10.1007/s00604-019-3379-8) contains supplementary material, which is available to authorized users.

✉ Fengli Qu
fengliquhn@hotmail.com

✉ Limin Lu
lulimin816@hotmail.com

[1] Key Laboratory of Crop Physiology, Ecology and Genetic Breeding, Ministry of Education, Institute of functional materials and agricultural applied chemistry, College of Science, Jiangxi Agricultural University, Nanchang 330045, People's Republic of China

[2] College of Chemistry and Chemical Engineering, Qufu Normal University, Qufu, Shandong 273165, People's Republic of China

[3] Department of Medicine, Soochow University, Suzhou, Jiangsu, China

the original properties of graphene, but also owns its unique adjustable pore structure, large specific surface area, good chemical and mechanical stability [11, 12]. Because of these intriguing characteristics, graphene aerogel has been deemed as a promising candidate material for the electroanalytical application, e.g., detection of quercetin [13] and H_2O_2 [14]. However, the widespread use of graphene aerogel as sensing material for microanalysis still faces several issues: firstly, graphene aerogel is a highly defect-free hydrophobic material, which shows poor interaction with the detection target [15]. Secondly, the inertness of the graphene sheets has led to graphene aerogel with an inactive property [16]. Thirdly, graphene aerogel shows high background current, which usually results in a low signal-to-noise ratio [17]. Hence, finding suitable modified materials to conquer these drawbacks of graphene aerogel is quite necessary.

Transition metal dichalcogenides (TMDs) have aroused extensive concern because of their intrinsic feature, such as graphene-like layered structure, high surface area, and superb electronical, photoelectron and electrocatalytic characteristics [18]. Among these TMDs, WS_2 is highly regarded owing to unparalleled electronic, optical, chemical, and physical properties [19]. Moreover, WS_2 with nanoscale has a greater effective surface area, more exposed active sites and better water solubility. Compared with bulk material, nanoscale WS_2 exhibits remarkable electrochemical performance due to its size effect [20]. Benefiting from these advantages, WS_2 is deemed as a promising decoration for carbon materials. For example, Yang et al. have reported the self-assembly of WS_2 onto reduced graphene oxide (rGO) and the composite showed an enhanced activity for the catalytic hydrogen evolution [21]. Liu et al. have synthesized the hybrids of WS_2 and carbon nanotube, which was demonstrated as an ultrasensitive electrochemical biosensor for DNA detection [22]. Although numerous works on the fabrication and application of WS_2/carbon composites have been reported, as far as we know, literatures on preparation of 3D WS_2 nanosheets/reduced graphene aerogel (WS_2/rGA) are relative few [23]. WS_2 nanosheets/rGA hybrid aerogels may be used as a promising electrode material. They can boost the detection performance because the hybrid aerogels combine the attractive characteristics of rGO sheets and WS_2 nanosheets, and the special properties of rGA.

Herein, 3D WS_2/rGA hybrid network was fabricated via a one-pot hydrothermal technique along with in-situ self-assembly procedure and was employed as electrode material for the determination of nitrite. The 3D porous interconnected network with huge specific area provided a perfect matrix to load WS_2 nanosheets and enhanced the exposed edge sites of WS_2. The unique WS_2-anchored-on-rGA structure endowed the composite with plentiful active sites, which facilitated the catalytic oxidation of nitrite. Also, the WS_2/rGA electrode showed a lower background signal than rGA electrode, resulting in a low detection limit of nitrite. In addition, the WS_2/rGA electrode revealed good selectivity and reproducibility, as well as excellent long-term stability towards electrochemical detection of nitrite.

Experimental section

Chemical materials and reagents

Graphene oxide (GO) was purchased from Nanjing XF Nano Co (Nanjing, China, www.xfnano.com). The lateral size of the GO is about 0.5~5 μm, and the thickness is about 0.8~1.2 nm. Na_2HPO_4, NaH_2PO_4, KCl, $K_3[Fe(CN)_6]$, and $K_4Fe(CN)_6$ were purchased from the Sigma-Aldrich (www.sigmaaldrich.com). Nitrite, N,N-dimethylformamide (DMF, ≥98%) and tungsten disulfide (WS_2) were purchased from Aladdin Chemistry Co. Ltd. (Shanghai, China, www.aladdin-e.com). Other reagents were of analytical grade and used as received.

Apparatus

The morphology of nanocomposites was performed by scanning electron microscopy (SEM) (Hitachi S4800, Japan). The X-ray photoelectron spectroscopy (XPS) data were collected on a Thermo Fisher Scientific using an Al Kα X-ray source. X-ray diffraction (XRD) pattern was measured on a Germany Bruker D8 X-ray diffractometer. All electrochemical measurements were studied by a computerized CHI660D electrochemical workstation from CH instruments (Shanghai, China). A traditional three-electrode system was established in the experiment, including saturated calomel reference electrode, platinum wire auxiliary electrode, and glassy carbon working electrode (GCE, $\phi = 3$ mm).

Synthesis of tungsten disulfide (WS_2) and its composite with reduced graphene oxide aerogel (WS_2/rGA)

Chemically exfoliated WS_2 nanosheets were synthetized by lithium intercalation [24]. Briefly, 0.6 g WS_2 was dispersed in a mixture of n-hexane (24 mL) and n-butyl lithium (6 mL). After that, the mixed solution was transferred to a 50 mL three-necked flask, and heated at 80 °C under a nitrogen atmosphere. 48 h later, the mixture was centrifuged at 8000 rpm and rinsed excess n-butyllithium with n-hexane for five times. The product was dried under vacuum for 0.5 h at room temperature, mixed with water to a 1.5 mg mL^{-1} WS_2, and ultrasonic for 20 min to obtain a homogeneous solution.

The WS_2/rGA composite was synthesized via hydrothermal technique by the following procedure. In a typical synthesis of WS_2/rGA, GO (40 mg) was dissolved in deionized

water (14 mL) and sonicated for 10 min to form homogeneous solution. Then, 6 mL of WS_2 solution (1 mg mL^{-1}) was added into GO solution. After 30 min of stirring, the mixture was transferred into 20 mL Teflon equipped autoclave, sealed and reacted at 180 °C for 12 h. After that, the autoclave was allowed to cool to room temperature. The product was freeze-dried at −50 °C for 12 h to remove water, and a porous internetwork structure was formed in this process.

Preparation of modified glassy carbon electrodes

2 mg WS_2/rGA composite was suspended in 2 mL DMF to obtain WS_2/rGA dispersion (1 mg mL^{-1}).

For the fabrication of modified electrode, bare glassy carbon electrodes (GCEs; ϕ = 3 mm) were firstly polished for 5 min by aluminum oxide to form a bright mirror surface, then the impurity was completely removed by ultrasonic with double distilled water. After drying, GCE was modified with 5 μL WS_2/rGA suspension. The WS_2/rGA modified electrode was dried under the infrared lamp. The synthesis process is illustrated in Scheme 1.

Electrochemical measurements

5 mL of phosphate buffer (PB) solution (0.1 M, pH 6.0) as the supporting electrolyte was used during all electrochemical experiments. Cyclic voltammetry (CV) measurement was carried out in the range of 0.3–1.1 V at a scan rate of 100 mV s^{-1}. Different pulse voltammetry (DPV) analysis was performed in the range of 0.2–1.2 V with a pulse period of 0.5 s, a pulse width of 0.05 s and the amplitude of 50 mV. Electrochemical impedance spectroscopy (EIS) was carried out in the mixture of 5 mM $[Fe(CN)_6]^{3-/4-}$ and 0.1 M KCl. The frequency range was 10^5 Hz to 1.0 Hz and the amplitude was 5 mV.

Real sample analyses

To assess the practical analytical utility of the designed WS_2/rGA electrode, electrochemical detection of nitrite in bacon was studied. The bacon was purchased from the local supermarket. 2 g of bacon sample was cut and dispersed into 10 mL 0.1 M PB solution (pH 6.0) buffer solution. The mixed solution was stirred for 20 min and then centrifuged for 10 min to remove impurities and obtain a clear solution. Electrochemical detection of nitrite in practical samples was carried out by using standard addition method. The content of nitrite in the actual sample was analyzed in the form of recovery.

Results and discussion

Characterization of WS_2 and WS_2/rGA materials

X-ray diffraction (XRD) is used to confirm the phase and crystal structure of rGA and WS_2/rGA. As shown in Fig. 1a, rGA presents a broad diffraction peak at 22.3°, which can be ascribed to (002) reflections of rGA, demonstrating the diffraction characteristics of graphene [25]. For the WS_2/rGA composite, the diffraction peaks exhibit at 2θ = 22.3°, 41.5° 46.8°, 65.4° and 71.3°, which correspond to the (002), (103), (006), (112) and (200) of WS_2, respectively (JCPDS-ICDD 87–2417), indicating the formation of WS_2 in the microstructure of rGA [26].

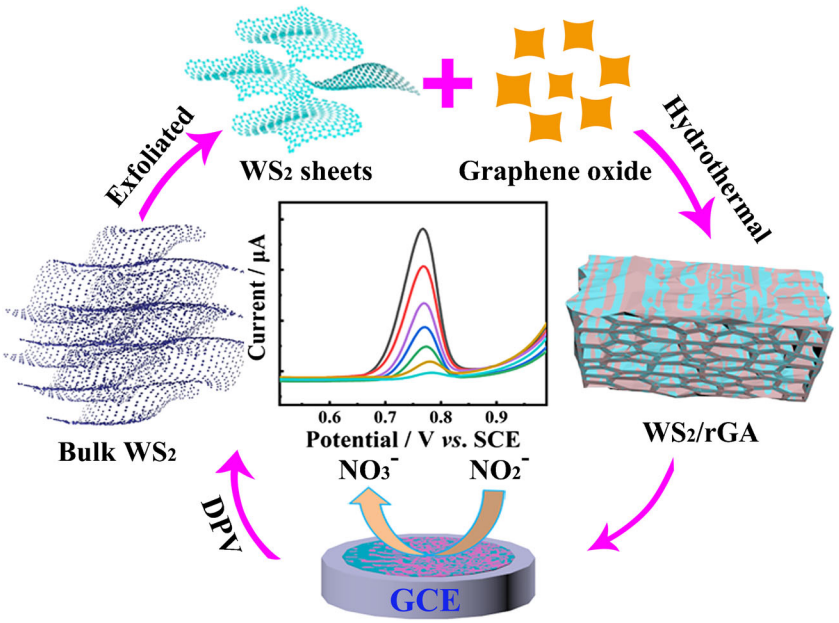

Scheme 1 Schematic presentation of the fabrication procedure of tungsten disulfide/reduced graphene oxide aerogel (WS_2/rGA) and the detection principle for nitrite

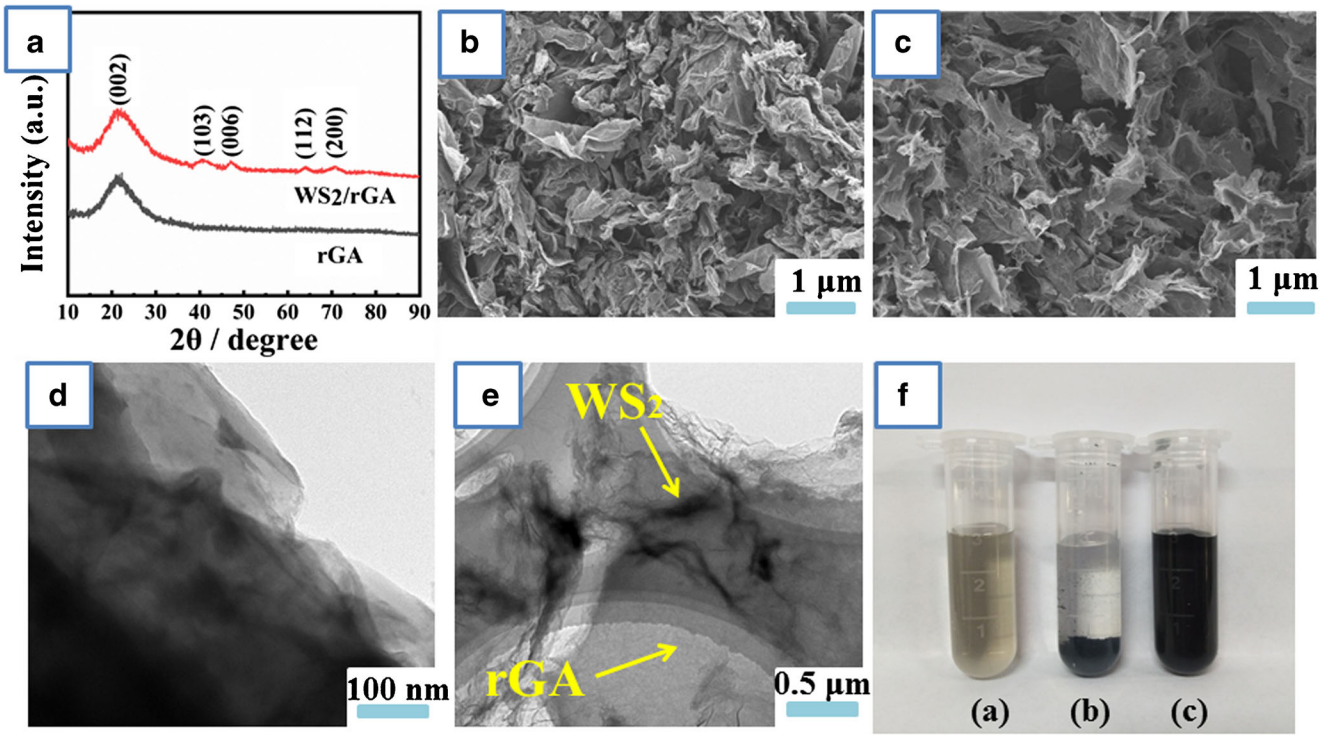

Fig. 1 XRD patterns of rGA and WS_2/rGA (**a**); SEM images of rGA (**b**) and WS_2/rGA (**c**); TEM images of WS_2 (**d**) and WS_2/rGA (**e**); Digital image (**f**) of WS_2 (a), rGA (b) and WS_2/rGA (c)

The surface morphologies of rGA and WS_2/rGA composite were characterized by scanning electron microscope (SEM). From Fig. 1b, it can be clearly seen that rGA exhibits an interconnected porous 3D framework, and is rich in hierarchical pores with a wide size distribution. After the self-assemble of WS_2 into rGA network (Fig. 1c), the composite appears to be much smoother and the pores became larger. In addition, the chemical constitution of WS_2/rGA composite was characterized by energy dispersive X-ray spectroscopy (EDS). As shown in Fig. S1, the W and S signals are from WS_2. The C and O signals are from rGO. To further investigate the microstructure of WS_2/rGA composite, Transmission electron microscope (TEM) analysis was then performed. As shown in Fig. 1d, WS_2 nanosheets with 2D layered structure are clearly observed. From the TEM of WS_2/rGA, we can see that WS_2 nanosheets are uniformly and tightly decorated on the surface of rGA.

Fig. 1f(a), (b) and (c) show the photographs of WS_2, rGA and WS_2/rGA, respectively. As shown, WS_2 sheets can be well dispersed in water (Fig. 1f(a)). However, rGA is completely settled down at the bottom of the vial (Fig. 1f(b)). By contrast, WS_2/rGA (Fig. 1f(c)) can be easily dispersed in water to form a dark suspension, demonstrating that the composite is hydrophilic.

The oxidation state and chemical composition of WS_2/rGA was characterized by X-ray Photoelectron Spectroscopy (XPS). For the spectrum of WS_2/rGA (Fig. 2a), it denotes four main peaks for W4f, S2p, C1s and O1s, which are located at 34.6, 168.9, 285.6 and 568.9 eV, respectively. Fig. 2b presents C1s spectrum of WS_2/rGA. As shown, three functional groups appear at 285.4, 286.6 and 288.8 eV, which are associated with C-C, C-O, and C=O, respectively. The binding energy of the S2p peak (Fig. 2c) appears at 167.9 and 170.6 eV, corresponding to $S2p_{3/2}$ and $S2p_{1/2}$, respectively [27]. W4f XPS spectra is shown in Fig. 2d. $W4f_{7/2}$ and $W4f_{5/2}$ are observed at 33.4 and 35.8 eV, respectively, indicating that the existence of W (VI) in WS_2.

Electrochemical characterization of the composite prepared from tungsten disulfide and reduced graphene oxide aerogel (WS_2/rGA)

Electrochemical impedance spectroscopy (EIS), an effective method was used to evaluate charge transfer on electrode surface [28]. The high frequency semicircle represents the resistance of the electron transfer (Ret), and the straight part represents the diffusion-limited process [29]. Fig. 3 shows the Nyquist diagrams of bare GCE (a), WS_2/GCE (b), rGA/GCE (c), and WS_2/rGA/GCE (d). As shown, bare GCE (a) exhibits a large semicircle. For WS_2/GCE (b), the Ret is larger than that of bare GCE, which can be attributed to the poor conductivity of WS_2 (b). Nevertheless, after rGA was decorated on bare GCE (c), the Ret is dramatically decreased, which is because that rGA with excellent electronic conductivity improves the electron transmission rate. Furthermore, for WS_2/rGA/GCE (d), the Ret is increased, which indicates the successful introduction of WS_2 into rGA.

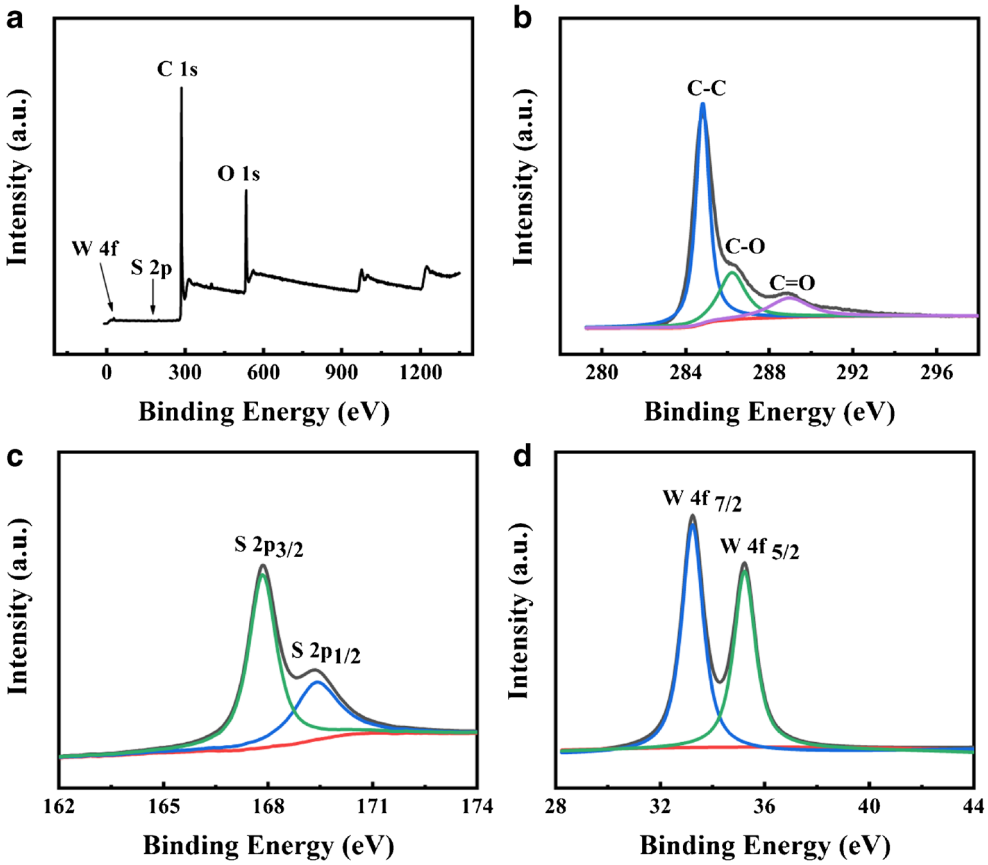

Fig. 2 XPS spectra of WS_2/rGA sample, including survey XPS spectrum (**a**), high resolution spectra of C1s (**b**), S2p (**b**) and W4f (**d**)

Electrochemical behavior of nitrite at different electrodes

Cyclic voltammetry (CV) experiments were performed to investigate the electrochemical behavior of 80.0 μM nitrite at bare GCE (a), WS_2/GCE (b), rGA/GCE (c) and WS_2/rGA/GCE (d) in 0.1 M PB solution (pH = 6.0) (Fig. 4a). As shown, bare GCE (a) and WS_2/GCE (b) show a relatively weak and irreversible oxidation peak due to the sluggish electron transfer kinetics of GCE and the poor conductivity of WS_2. However, for rGA/GCE (c), the anodic peak current increases dramatically associated with a negative shift in the peak potential, which is because that the high electron transfers rate and the 3D architecture of rGA accelerate the electrochemical oxidation of nitrite. Moreover, the WS_2/rGA/GCE (d) shows a much higher peak oxidation along with a lower background

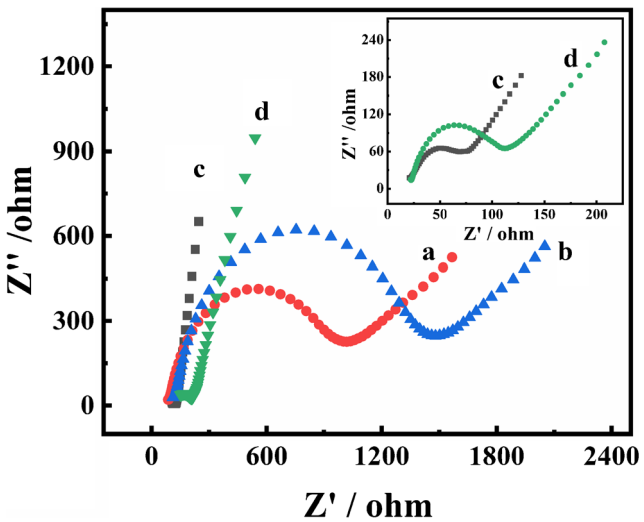

Fig. 3 EIS of different modified electrodes bare GCE (**a**), WS_2/GCE (**b**), rGA/GCE (**c**) and WS_2/rGA/GCE (**d**) in the supporting electrolyte of 0.1 M KCl solution containing 5.0 mM of $[Fe(CN)_6]^{3-/4-}$

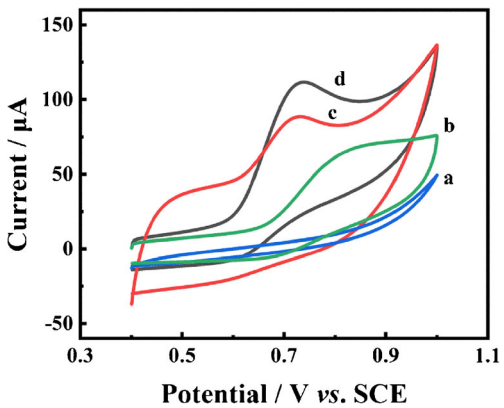

Fig. 4 CV response of different electrodes including bare GCE (**a**), WS_2/GCE (**b**), rGA/GCE (**c**) and WS_2/rGA/GCE (**d**) in 0.1 M PB solution (pH 6.0) containing 80.0 μM nitrite at a scan rate of 100 mV s^{-1}

current in comparison with rGA/GCE (c). The observed enhancement in the anodic peak current as well as lowering of background current can be attributed to the synergistic effect between rGA and WS_2. rGA serves as a scaffold and support for the dispersion of WS_2 nanosheets and the loaded WS_2 affords more active edge sites, thereby increasing the electro-catalytic activity of the composite electrode for the nitrite oxidation.

Optimization of experimental conditions

The influence of different pH values (3.0~8.0) on the nitrite oxidation peak current (80.0 μM) was investigated. As observed from Fig. S2, the response current increases with increasing pH from 3.0 to 6.0, and maximizes at pH 6.0. The reason for this phenomenon is attributed to the fact that nitrite can be easily decomposed to nitric oxide and nitrate in strongly acidic solution [30]. When pH is higher than 7.0, the oxidation peak current gradually decreases, demonstrating the oxidation of nitrite became more difficult because of the lack of protons [31]. Therefore, PB solution with pH of 6.0 is chosen as electrolyte in subsequent experiments.

Effect of scan rate

The kinetic characteristic for the nitrite oxidation reaction at WS_2/rGA electrode was studied by CV experiments at different scanning rates. As shown in Fig. 5a, the peak current increases as the scan rate increases from 30 mV s^{-1} to 210 mV s^{-1}. Moreover, the oxidation peak current is proportional to the scan rates (Fig. 5b). The linear equation is described as I (μA) = 29.730 + 0.333 v (mV s^{-1}) (R^2 = 0.992). The result indicates that the electrochemical oxidation of nitrite on WS_2/rGA/GCE surface is a diffusion control process. Moreover, the oxidation peak currents and the square root of the scan rate have a satisfactory linear relationship (Fig. 5c). The linear equation is I = −2.335 + 6.801 $v^{1/2}$, (R^2 = 0.998), which also suggests that the oxidation of nitrite on WS_2/rGA modified electrode is a diffusion control process.

Analytical performance

Under optimal conditions, the quantitative analysis of nitrite on WS_2/rGA/GCE was carried out by differential pulse voltammetry (DPV). As presented in Fig. 6, the anode peak of nitrite is observed at about 0.68 V and the peak current is enhanced gradually with the increase of nitrite concentration. From the inset of Fig. 6, the oxidation peak currents exhibit a good linear relationship with nitrite concentrations in the range from 0.0100 μM to 130 μM. The linear equations can be described as I (μA) = 2.734 + 0.323 c (μM) (R^2 = 0.997). The detection limit is estimated to be 3 nM on the basis of S/N = 3 [32, 33]. The analytical performance of the WS_2/rGA electrode is compared with other published results (Table 1). It

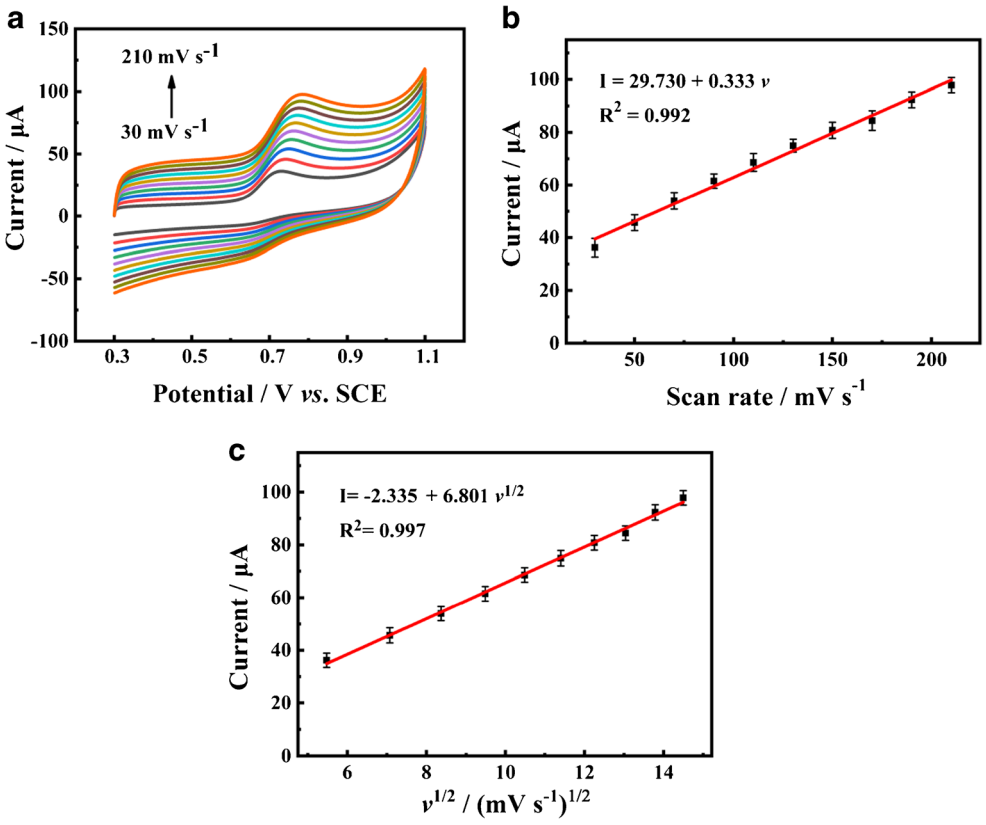

Fig. 5 **a** CV curve for WS_2/rGA/GCE at different scan rates from 30 mV s^{-1} to 210 mV s^{-1} in 0.1 M PB solution (pH 6.0) containing 100.0 μM nitrite; **b** Linear relation of scan rates *vs.* oxidation peak current; **c** The plots of the oxidation peak currents *vs.* the square root of the scan rate (I ~ $v^{1/2}$)

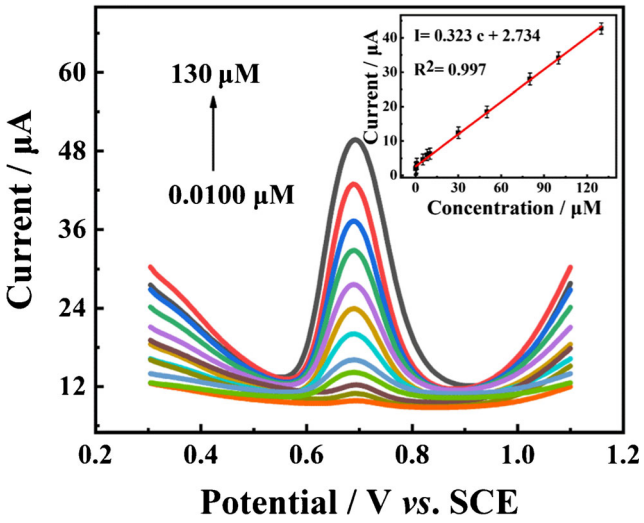

Fig. 6 DPVs of WS_2/rGA/GCE in 0.1 M PB solution (pH = 6.0) for different nitrite concentrations in the range of 0.0100, 0.0500, 0.300, 0.500, 0.800, 5.00, 8.00, 10.0, 30.0, 50.0, 80.0, 100 to 130 μM. Inset: Plots of oxidation currents versus the concentration of nitrite

is found that the present WS_2/rGA electrode shows a lower detection limit. This can be attributed to the following several aspects: firstly, 3D architectural rGA shows large specific surface area, which is propitious to the loading of WS_2. Secondly, the WS_2 sheets attached on rGA provide plentiful active sites, and thus the electro-catalytic properties of composites are enhanced.

Selectivity, reproducibility and stability

The selectivity of the fabricated WS_2/rGA modified electrode for the determination of nitrite was investigated. Electrochemical results show that the current response of 100.0 μM nitrite at WS_2/rGA modified electrode has no obviously influence by the addition of 50-fold K^+, Na^+, Zn^{2+}, Ca^{2+}, Cl^-, NO_3^-, SO_4^{2-} or CO_3^{2-}. The result shows that the peak current change is less than 5%, which suggests the good selectivity of the created WS_2/rGA modified electrode toward the determination of nitrite.

To test the practicality of the created WS_2/rGA modified electrode, five independently electrodes were used to detect 100.0 μM nitrite and the RSD was about 3.7%, which illustrates that the WS_2/rGA/GCE has a favorable reproducibility. Furthermore, the long-term stability of WS_2/rGA/GCE was evaluated over 2 weeks' period and the response toward 100.0 μM nitrite was monitored every 2 days. The change of the peak current for nitrite is almost negligible, indicating that the constructed WS_2/rGA electrode has a good stability.

Real sample determination for nitrite

To validate the effectiveness of the fabricated approach, WS_2/rGA/GCE was applied for the electrochemical detection of nitrite in bacon samples. 2 g of samples were pretreated to give a clear solution and stored in a 4 °C refrigerator. Quantitative analysis was carried out by adding a known concentration of nitrite to the sample solution. Each sample was tested for five times in parallel and then averaged. The corresponding test results are listed in Table S1. As shown, the recovery is in the range of 97.46–104.2% and the RSDs for the current response are less than 5%. These results suggest the WS_2/rGA electrode have great application prospect. To further evaluate the accuracy of the WS_2/rGA electrode, the result was compared with that from high performance liquid chromatography (HPLC). As shown in Table S1, the results from our designed method are in good agreement with HPLC method. As expected, the designed method can be applied to determine the nitrite concentration in real samples.

Conclusion

We have designed a novel WS_2/rGA electrode for nitrite detection based on 3D WS_2/rGA hybrid aerogel electrode

Table 1 Performance comparison of WS_2/rGA/GCE for detection of nitrite over various modified electrodes

Electrode	Linear range (μM)	LOD (nM)	Reference
α-Fe_2O_3 NAs/CF[a]	0.5–1000	120	[34]
Cu/Ag/MWNTs/GCE	1–1000	200	[35]
Cu/MWCNTs/GCE	5–1260	1800	[31]
Poly(TazoCoPc)/CNP[b]/GCE	0.02–1	6	[36]
c-MWCNT/TiN[c]/GCE	0.006–950	4	[37]
Chit-TsCuPc[d]/GCE	0.0005–0.065	2.2	[38]
WS_2/rGA/GCE	0.0100–130	3	This work

[a] α-Fe_2O_3 NAs/CF: α-Fe_2O_3 nanorod arrays/carbon foam

[b] Poly(TazoCoPc)/CNP: polymeric phthalocyanine

[c] c-MWCNT/TiN: carboxylated multiwalled carbon nanotubes/titanium nitride

[d] Chit-TsCuPc: copper phthalocyanine

material, which was synthesized through a hydrothermal method of mixing solvothermal. WS_2 nanosheets were well decorated on the porous network. The hybrid aerogel exhibited good 3D porous network, large active specific surface area and a great many active site, which enable it high catalytic activity toward nitrite oxidation. The WS_2/rGA composite as electrochemical platform showed wide detection range, low detection limit and high selectivity toward the determination of nitrite. The WS_2/rGA electrode can be used to detect nitrite in real samples with suitable recovery values.

Acknowledgements We are grateful to the National Natural Science Foundation of China (21665010, 51862014, 31741103, 51302117), the outstanding youth fund of Jiangxi Province (20162BCB23027), the Natural Science Foundation of Jiangxi Province (20171BAB203015) for their financial support of this work.

Compliance with ethical standards The author(s) declare that they have no competing interests.

References

1. Li L, Liu D, Wang K, Mao H, You T (2017) Quantitative detection of nitrite with N-doped graphene quantum dots decorated N-doped carbon nanofibers composite-based electrochemical sensor. Sensors Actuators B Chem 252:17–23
2. Chen SS, Shi YC, Wang AJ, Lin XX, Feng JJ (2017) Free-standing Pt nanowire networks with clean surfaces: highly sensitive electrochemical detection of nitrite. J Electroanal Chem 791:131–137
3. Jian JM, Fu L, Ji J, Lin L, Guo X, Ren TL (2018) Electrochemically reduced graphene oxide/gold nanoparticles composite modified screen-printed carbon electrode for effective electrocatalytic analysis of nitrite in foods. Sensors Actuators B Chem 262:125–136
4. Zhao J, Lu Y, Fan C, Wang J, Yang Y (2015) Development of a cloud point extraction and spectrophotometry-based microplate method for the determination of nitrite in human urine and blood. Spectrochim Acta A 136:802–807
5. Wang XF, Fan JC, Ren R, Jin Q, Wang J (2016) Rapid determination of nitrite in foods in acidic conditions by high-performance liquid chromatography with fluorescence detection. J Sep Sci 39: 2263–2269
6. Lin Z, Xue W, Chen H, Lin JM (2011) Peroxynitrous-acid-induced chemiluminescence of fluorescent carbon dots for nitrite sensing. Anal Chem 83:8245–8251
7. Ikhsan NI, Rameshkumar P, Pandikumar A, Mehmood Shahid M, Huang NM, Vijay Kumar S, Lim HN (2015) Facile synthesis of graphene oxide-silver nanocomposite and its modified electrode for enhanced electrochemical detection of nitrite ions. Talanta 144: 908–914
8. Jijie R, Kahlouche K, Barras A, Yamakawa N, Bouckaert J, Gharbi T, Szunerits S, Boukherroub R (2018) Reduced graphene oxide/polyethylenimine based immunosensor for the selective and sensitive electrochemical detection of uropathogenic Escherichia coli. Sensors Actuators B Chem 260:255–263
9. Wang X, Chen Y, Zheng B, Qi F, He J, Li P (2016) Few-layered WSe_2 nanoflowers anchored on graphene nanosheets: a highly efficient and stable electrocatalyst for hydrogen evolution. Electrochim Acta 222:1293–1299
10. Lu L (2018) Recent advances in synthesis of three-dimensional porous graphene and its applications in construction of electrochemical (bio)sensors for small biomolecules detection. Biosens Bioelectron 110:180–192
11. Yang L, Li Y, Zhang Y, Fan D, Pang X, Wei Q, Du B (2017) 3D nanostructured palladium-functionalized graphene-aerogel-supported Fe_3O_4 for enhanced $Ru(bpy)_3^{2+}$-based Electrochemiluminescent Immunosensing of prostate specific antigen. ACS Appl Mater Interfaces 9:35260–35267
12. Qiu B, Xing M, Zhang J (2018) Recent advances in three-dimensional graphene based materials for catalysis applications. Chem Soc Rev 47:2165–2216
13. Niu X, Li X, Chen W, Li X, Weng W, Yin C, Dong R, Sun W, Li G (2018) Three-dimensional reduced graphene oxide aerogel modified electrode for the sensitive quercetin sensing and its application. Mater Sci Eng C Mater 89:230–236
14. Chen L, Wang X, Zhang X, Zhang H (2012) 3D porous and redox-active prussian blue-in-graphene aerogels for highly efficient electrochemical detection of H_2O_2. J Mater Chem 22:22090–22096
15. Cheng Y, Tan M, Hu P, Zhang X, Sun B, Yan L (2018) Strong and thermostable SiC nanowires/graphene aerogel with enhanced hydrophobicity and electromagnetic wave absorption property. Appl Surf Sci 448:138–144
16. Guo D, Lu Y, Zhao Y, Zhang Y (2015) Synthesis and physicochemical properties of graphene/ZrO_2 composite aerogels. RSC Adv 5: 11738–11744
17. Wu S, Fan S, Tan S, Wang J, Li CP (2018) A new strategy for the sensitive electrochemical determination of nitrophenol isomers using β-cyclodextrin derivative-functionalized silicon carbide. RSC Adv 8:775–784
18. Wang Y, Ma J, Ye X, Wong WL, Li C, Wu K (2018) Enhanced effects of ionic liquid and gold nanoballs on the photoelectrochemical sensing performance of WS_2 nanosheets towards 2,4,6-tribromophenol. Electrochim Acta 271:551–559
19. Ratha S, Rout CS (2013) Supercapacitor electrodes based on layered tungsten disulfide-reduced graphene oxide hybrids synthesized by a facile hydrothermal method. ACS Appl Mater Interfaces 5:11427–11433
20. Yu H, Zhu H, Dargusch M, Huang Y (2018) A reliable and highly efficient exfoliation method for water-dispersible MoS_2 nanosheet. J Colloid Interface Sci 514:642–647
21. Yang J, Voiry D, Ahn SJ, Kang D, Kim AY, Chhowalla M, Shin HS (2013) Two-dimensional hybrid nanosheets of tungsten disulfide and reduced graphene oxide as catalysts for enhanced hydrogen evolution. Angew Chem 125:13996–13999
22. Liu X, Shuai HL, Liu YJ, Huang KJ (2016) An electrochemical biosensor for dna detection based on tungsten disulfide/multi-walled carbon nanotube composites and hybridization chain reaction amplification. Sensors Actuators B Chem 235:603–613
23. Yan W, Worsley MA, Pham T, Zettl A, Carraro C, Maboudian R (2018) Effects of ambient humidity and temperature on the NO_2 sensing characteristics of WS_2 /graphene aerogel. Appl Surf Sci 450:372–379
24. Liang A, Li D, Zhou W, Wu Y, Ye G, Wu J, Chang Y, Wang R, Xu J, Nie G, Hou J, Du Y (2018) Robust flexible WS_2/PEDOT:PSS film for use in high-performance miniature supercapacitors. J Electroanal Chem 824:136–146
25. Wang Y, Jin Y, Pan E, Jia M (2018) Fe_3O_4 nanoparticle/graphene aerogel composite with enhanced lithium storage performance. Appl Surf Sci 458:1035–1042
26. Parsaei M, Asadi Z, Khodadoust Z (2015) A sensitive electrochemical sensor for rapid and selective determination of nitrite ion in water samples using modified carbon paste electrode with a newly synthesized cobalt(II)-Schiff base complex and magnetite nanospheres. Sensors Actuators B Chem 220:1131–1138

27. Sun T, Li Z, Liu X, Ma L, Wang J, Yang S (2016) Facile construction of 3D graphene/MoS_2 composites as advanced electrode materials for supercapacitors. J Power Sources 331:180–188
28. Zhou Y, Yang L, Li S, Dang Y (2017) A novel electrochemical sensor for highly sensitive detection of bisphenol a based on the hydrothermal synthesized Na-doped WO_3 nanorods. Sensors Actuators B Chem 245:238–246
29. Thangavelu K, Raja N, Chen SM, Liao WC (2017) Nanomolar electrochemical detection of caffeic acid in fortified wine samples based on gold/palladium nanoparticles decorated graphene flakes. J Colloid Interface Sci 501:77–85
30. Ghaneimotlagh M, Taher MA (2018) A novel electrochemical sensor based on silver/halloysite nanotube/molybdenum disulfide nanocomposite for efficient nitrite sensing. Biosens Bioelectron 109:279–285
31. Manoj D, Saravanan R, Santhanalakshmi J, Agarwal S, Gupta VK, Boukherroub R (2018) Towards green synthesis of monodisperse cu nanoparticles: an efficient and high sensitive electrochemical nitrite sensor. Sensors Actuators B Chem 266:873–882
32. Committee AM (1987) Recommendations for the definition, estimation and use of the detection limit. Analyst 112:199–204
33. Armbruster DA, Tillman MD, Hubbs LM (1994) Limit of detection (LQD)/limit of quantitation (LOQ): comparison of the empirical and the statistical methods exemplified with GC-MS assays of abused drugs. Clin Chem 40:1233–1238
34. Ma Y, Song X, Ge X, Zhang H, Wang G, Zhang Y (2017) In situ growth of α-Fe_2O_3 nanorod arrays on 3D carbon foam as an efficient binder-free electrode for highly sensitive and specific determination of nitrite. J Mater Chem A 5:4726–4736
35. Zhang Y, Nie J, Wei H, Xu H, Wang Q, Cong Y (2017) Electrochemical detection of nitrite ions using ag/cu/MWCNT nanoclusters electrodeposited on a glassy carbon electrode. Sensors Actuators B Chem 258:1107–1116
36. Aralekallu S, Mohammed I, Manjunatha N, Palanna M, Sannegowda LK (2019) Synthesis of novel azo group substituted polymeric phthalocyanine for amperometric sensing of nitrite. Sensors Actuators B Chem 282:417–425
37. Annalakshmi M, Balasubramanian P, Chen SM, Chen TW (2019) Amperometric sensing of nitrite at nanomolar concentrations by using carboxylated multiwalled carbon nanotubes modified with titanium nitride nanoparticles. Microchim Acta 186:8
38. Sudarvizhi A, Pandian K, Oluwafemi OS, Gopinath SC (2018) Amperometry detection of nitrite in food samples using tetrasulfonated copper phthalocyanine modified glassy carbon electrode. Senors Actuators B 272:151–159